Correlations in the Motion of Atoms in Liquid Argon*

A. RAHMAN
Argonne National Laboratory, Argonne, Illinois
(Received 6 May 1964)

A system of 864 particles interacting with a Lennard-Jones potential and obeying classical equations of motion has been studied on a digital computer (CDC 3600) to simulate molecular dynamics in liquid argon at 94.4°K and a density of 1.374 g cm^{-3}. The pair-correlation function and the constant of self-diffusion are found to agree well with experiment; the latter is 15% lower than the experimental value. The spectrum of the velocity autocorrelation function shows a broad maximum in the frequency region $\omega=0.25(k_BT/\hbar)$. The shape of the Van Hove function $G_s(r,t)$ attains a maximum departure from a Gaussian at about $t=3.0\times10^{-12}$ sec and becomes a Gaussian again at about 10^{-11} sec. The Van Hove function $G_d(r,t)$ has been compared with the convolution approximation of Vineyard, showing that this approximation gives a too rapid decay of $G_d(r,t)$ with time. A delayed-convolution approximation has been suggested which gives a better fit with $G_d(r,t)$; this delayed convolution makes $G_d(r,t)$ decay as t^4 at short times and as t at long times.

I. INTRODUCTION

In recent years considerable use has been made of large digital computers to study various aspects of molecular dynamics in solids, liquids, and gases.[1] The following is a description of a computer experiment on liquid argon (using the CDC 3600) to study the space and time dependence of two-body correlations which determine the manner in which slow neutrons are inelastically scattered from the liquid. If neutron scattering data of unlimited accuracy and completeness was available, then the kind of work presented here would serve the useful though unexciting purpose of confirming the results already obtained with neutrons. At present, however, the situation is that theorists are trying to build models for these two-body dynamical correlations to account for the observed neutron spectra; the current interest in the work presented here is thus to throw some light on the validity of these models, and to suggest the manner in which some improvements can be made.

The calculations presented here are based on the assumption that classical dynamics with a two-body central-force interaction can give a reasonable description of the motion of atoms in liquid argon. For practical reasons, further assumptions have to be made, namely, the interaction potential has to be truncated beyond a certain range, the number of particles in the assembly has to be kept rather small, and suitable boundary conditions have to be imposed on the assembly. Finally, the equations of motion have to be solved as a set of difference equations, thus involving a certain increment of time to go from one set of positions and velocities to the next. The details will be set forth in the next section. At the end of the paper a brief mention will be made of checks on the validity of these assumptions. The results presented in this paper are confined mainly to one pair of values of the temperature and the density of the system, namely, 94.4°K and 1.374 g cm^{-3}. A less exhaustive study, at 130°K and 1.16 g cm^{-3}, is mentioned briefly at the end.

II. METHOD OF COMPUTATION

The calculations reported here were based on the following ingredients.

Particles with mass $39.95\times1.6747\times10^{-24}$ g (the mass of an argon atom) were assumed to interact in pairs according to the potential $V(r)=4\epsilon\{(\sigma/r)^{12}-(\sigma/r)^6\}$, $\epsilon/k_B=120$°K, $\sigma=3.4$ Å, r being the distance between the particles. This interaction was assumed to extend up to a range $R=2.25\sigma$, so that a particle interacts with all particles situated within a sphere of that radius; $V(2^{1/6}\sigma)=-\epsilon$ is the minimum of $V(r)$ and at $r=R$, $V\sim-0.03\epsilon$.

864 such particles were placed in arbitrary positions in a cubical box of side $L=10.229\sigma$, thus providing a density of 1.374 g cm^{-3}. Periodic boundary conditions were imposed, so that at any given moment a particle with coordinates x, y, z inside the real box implied the presence of 26 periodic images with coordinates obtained by adding or subtracting L from each Cartesian coordinate. The density was conserved because when a particle moves out across one face of the cube another moves in across the opposite face.

The particles were then allowed to move, and their motions were calculated using a set of difference equations with a time increment of 10^{-14} sec. The details have been given in an Appendix. The positions and velocities obtained at successive moments were recorded on magnetic tape for later analysis. The only quantity monitored during the progress of the calculation was the mean-square velocity of the particles expressed in temperature units,

$$T=\frac{M}{3Nk_B}\sum_{i=1}^{N}\mathbf{v}_i^2,$$

where $N=864$. In the initial stages of the calculation, if T was not in the region of temperature (90°K) at which the system was to be studied, all velocities were

* Based on work performed under the auspices of the U. S. Atomic Energy Commission.
[1] J. R. Beeler, Jr., in *Physics of Many-Particle Systems*, edited by E. Meeron (Gordon and Beach Publishers, Inc., New York, 1964).

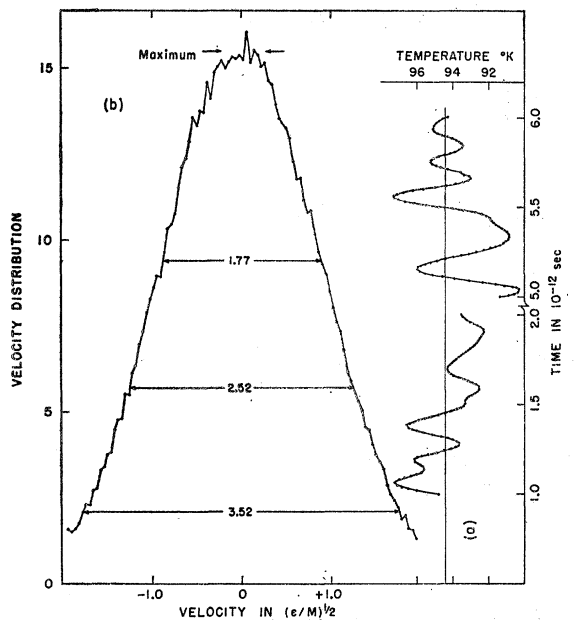

FIG. 1. Fluctuations of temperature with time in two sample regions (curve a); distribution of velocities is shown as curve b; widths of the distribution are shown at $e^{-1/2}$, e^{-1}, and e^{-2} of maximum.

stepped up or down by a constant factor and the system again left to follow its course.

At the completion of one such "experiment," the tape containing the record of positions and velocities was analyzed for the time-independent and time-dependent correlations. For the former, the information at each time can be analyzed without reference to the information at other times, and the correlations calculated at different times can be assembled into one ensemble average. For time-dependent correlations, any moment can be considered as the time origin, and again an ensemble average can be made with a succession of time origins.

The time-independent correlations investigated were the distribution of velocities and the pair-distribution function $g(r)$; if $n(r)$ particles are situated at a distance between r and $r+\Delta r$ from a given particle we have

$$g(r)=(V/N)[n(r)/4\pi r^2\Delta r].$$

The time-dependent correlations investigated were: (i) The mean values of the even powers of the displacements $\langle r^{2n}\rangle$, given by

$$\langle r^{2n}\rangle=\frac{1}{N}\sum_{i=1}^{N}[\mathbf{r}_i(t)-\mathbf{r}_i(0)]^{2n},\quad n=1,2,3,4.$$

We define a function[2] $G_s(r,t)$ which gives the probability of a particle attaining a displacement r in time t. We then have

$$\langle r^{2n}\rangle=\int r^{2n}G_s(r,t)d\mathbf{r}.$$

TABLE I. Mean temperature and the rms deviation after ν increments of time have been calculated. The value of the increment $=10^{-14}$ sec.

ν	$\bar{T}$ (°K) for Steps 1 to ν	$(\langle T^2\rangle_{\text{av}}-\bar{T}^2)^{1/2}/\bar{T}$
100	94.64	0.0167
200	94.47	0.0161
300	94.55	0.0158
400	94.55	0.0155
500	94.67	0.0160
600	94.51	0.0170
700	94.43	0.0170
780	94.45	0.0165

(ii) The velocity autocorrelation function, $\langle\mathbf{v}(0)\cdot\mathbf{v}(t)\rangle$, given by

$$\langle\mathbf{v}(0)\cdot\mathbf{v}(t)\rangle=\frac{1}{N}\sum_{i=1}^{N}\mathbf{v}_i(0)\cdot\mathbf{v}_i(t).$$

(iii) The time-dependent pair correlation function[2] $G_d(r,t)$; if at time t, $n(r,t)$ particles are situated at a distance between r and $r+\Delta r$ from the position which was occupied by a certain atom at $t=0$ then we define

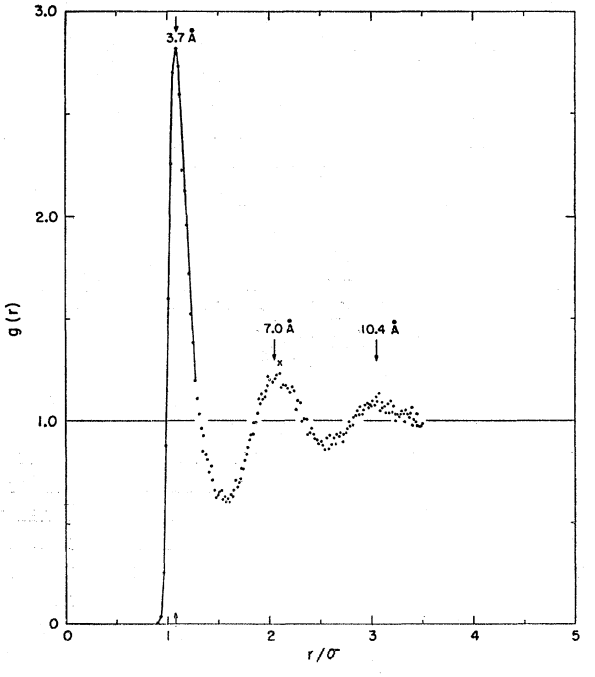

FIG. 2. Pair-correlation function obtained in this calculation at 94.4°K and 1.374 gcm^{-3}. The Fourier transform of this function has peaks at $\kappa\sigma=6.8$, 12.5, 18.5, 24.8.

[2] The functions G_s and G_d defined here are closely related to but not identical with, the Van Hove functions [L. Van Hove, Phys. Rev. **95**, 249 (1954)] G_s and G_d; for a discussion of this relationship see R. Aamodt, K. M. Case, M. Rosenbaum, and P. F. Zweifel [Phys. Rev. **126**, 1165 (1962)] and A. Rahman [Phys. Rev. **130**, 1334 (1963)].

this function as

$$G_d(r,t)=\frac{V}{N}\frac{n(r,t)}{4\pi r^2\Delta r}.$$

The suffix d, for "distinct," indicates that in this counting process the particle originally at the origin is excluded. We may remark here that $G_d(r,t)$ gives the time decay of the pair correlation, $g(r)$, which is identical with $G_d(r,0)$.

III. RESULTS

Figure 1(a) shows the fluctuation of temperature with the passage of time. The figure shows only two sample regions extending from step 100 to step 200 and from step 500 to step 600. A more complete analysis is given in Table I, which shows the mean the rms deviation relative to the mean.

The table shows that the mean remains steady, and we have adopted the value 94.4°K as the temperature of the system.

Figure 1(b) shows the distribution of velocities and the widths w_1, w_2, w_3 of the distribution at heights of $e^{-1/2}$, e^{-1}, and e^{-2} of the maximum. In a Maxwellian distribution we should have $w_2=2(2k_BT/\epsilon)^{1/2}$ [if the velocities are expressed in units of $(\epsilon/M)^{1/2}$] and $w_1=w_2/2^{1/2}=w_3/2$. At $T=94.4$°K, the numerical values of w_1, w_2, w_3 should be 1.78, 2.51, and 3.55, whereas in Fig. 1(b) they are 1.77, 2.52, and 3.52, respectively.

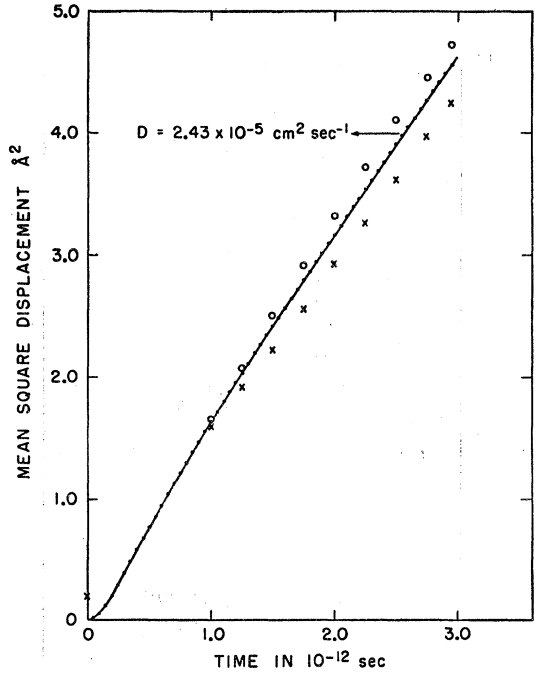

FIG. 3. Mean-square displacement of particles. The continuous curve is the mean of a set of 64 curves; the two members of the set which have *maximum* departures from the mean are shown as circles and as crosses. The asymptotic form of the continuous curve is $6Dt+C$, with D as shown on the figure and $C=0.2$ Å².

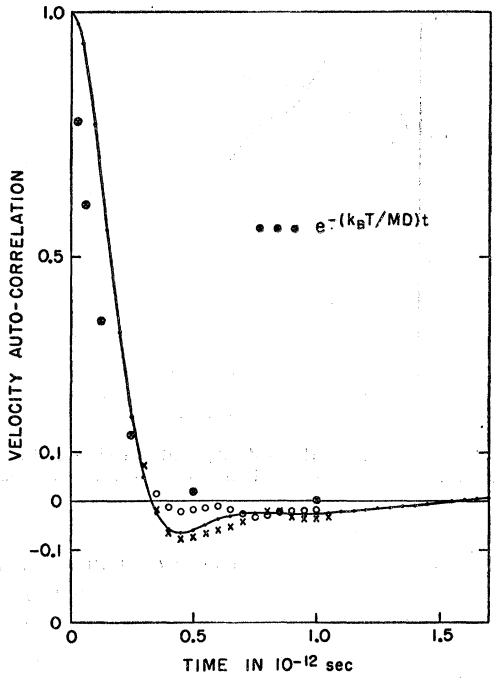

FIG. 4. The velocity autocorrelation function. The Langevin-type exponential function is also shown. The continuous curve, the circles, and the crosses correspond to the curves shown in Fig. 3.

Figure 2 shows $g(r)$ the pair distribution function. Using x rays, Eisenstein and Gingrich[3] have obtained $g(r)$ (at 91.8°K and 1.8-atm pressure) and the agreement with the $g(r)$ shown in Fig. 2 is quite satisfactory. To get a further check we have also calculated the transform of our $g(r)$, namely, the function

$$\gamma(\kappa)=\int_0^\infty \frac{\sin\kappa r}{\kappa r}\left\{\frac{N}{V}[g(r)-1]\right\}4\pi r^2dr.$$

The transform has peaks at $\kappa\sigma=6.8$, 12.5, 18.5, 24.8, whereas the peaks in the x-ray scattering[3] occur at $\kappa\sigma=6.8$, 12.3, 18.4, 24.4, respectively.

Figure 3 shows the mean-square displacement $\langle r^2\rangle$ obtained by averaging over an ensemble of 64 curves with as many different origins of time. Two *extreme* members of the set are also shown in Fig. 3 to exhibit the degree to which individual members of the set differ from their average. One can thus say that $\langle r^2\rangle$ written equivalently as $\langle r^2\rangle=(1/N)\sum(\mathbf{r}_i(t_0+t)-\mathbf{r}_i(t_0))^2$ is independent of the origin t_0, as it should be for a system in equilibrium.

From Fig. 3, it is seen that the asymptotic behavior $6Dt+C$ of $\langle r^2\rangle$ is already achieved at about $t\sim10^{-12}$ sec. At $t=2.5\times10^{-12}$ sec, its value is 3.9 Å² so that the rms displacement at that time is only about half the first-neighbor distance (3.7 Å). Thus, even after 2.5×10^{-12} sec we would expect that the identity of the first

[3] A. Eisenstein and N. S. Gingrich, Phys. Rev. **62**, 261 (1942).

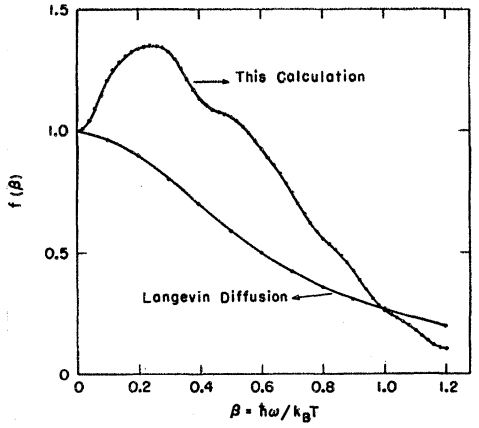

FIG. 5. Spectrum of the velocity autocorrelation function. The Lorentzian spectrum of a Langevin-type correlation is also shown.

neighbors is not completely lost. We shall see a more quantitative indication of this fact further below.

From the slope of the linear part of the curve for $\langle r^2\rangle$ one finds the diffusion constant D to be 2.43×10^{-5} cm^2 sec^{-1}; the temperature of our system is 94.4°K and the density is 1.374 g cm^{-3}; the experimental value of Naghizadeh and Rice,[4] for argon at 90°K and 1.374 g cm^{-3} is also 2.43×10^{-5} cm^2 sec^{-1}. The agreement thus is quite good.

Figure 4 shows the velocity autocorrelation function, $\langle \mathbf{v}(0)\cdot\mathbf{v}(t)\rangle$, normalized to unity at $t=0$ by dividing by $\langle \mathbf{v}^2\rangle$. Notice that the correlation becomes negative at $t=0.33\times10^{-12}$ sec and remains essentially negative as it goes to zero. In this respect it is radically different from the Langevin type of velocity autocorrelation, namely, $\exp(-k_BTt/MD)$, which is also shown in Fig. 4. A more illuminating way of exhibiting this qualitative difference is to consider the Fourier transform of the correlation, defined as

$$f(\omega)=\frac{kT}{MD}\int_0^\infty \frac{\langle \mathbf{v}(0)\cdot\mathbf{v}(t)\rangle}{\langle \mathbf{v}^2\rangle}\cos\omega t dt,$$

so that $f(0)=1.0$. Writing $\beta=\hbar\omega/k_BT$, $\lambda=\hbar/MD$, and $u=tk_BT/\hbar$, we get

$$f(\beta)=\lambda\int_0^\infty \frac{\langle \mathbf{v}(0)\cdot\mathbf{v}(u)\rangle}{\langle \mathbf{v}^2\rangle}\cos\beta u du.$$

Figure 5 shows $f(\beta)$ obtained from the correlation shown in Fig. 4; it has a broad maximum at about $\beta=0.25$. The transform of a Langevin-type correlation is a Lorentzian $\lambda^2/(\lambda^2+\beta^2)$ which is also shown in Fig. 5.

The time-dependent pair-correlation function, $G_d(r,t)$, was calculated for values of t ranging from 0 to 3.0×10^{-12} sec at intervals of 0.1×10^{-12} sec. It is shown in Fig. 6(a) for $t=10^{-12}$ sec and in Fig. 6(b) for $t=2.5\times10^{-12}$ sec. [$G_d(r,t=0)$ is the static pair distribution, $g(r)$, shown in Fig. 2.] It is seen that even at $t=2.5\times10^{-12}$ sec the remnants of the first-neighbor shell in $g(r)$ are visible.

This remark about the persistence of short-range correlations with the passage of time is relevant if one tries to describe the behavior of the liquid as quasi-crystalline. Whereas the increase of $\langle r^2\rangle$ with time (see Fig. 3) shown no such behavior, the function $\langle \mathbf{v}(0)\cdot\mathbf{v}(t)\rangle$ does show such a behavior, through that of its transform $f(\beta)$ which has a maximum reminiscent of the maximum in the frequency spectrum of a solid; moreover, the short-range order in the arrangement of an atom and its neighbors also shows a certain degree of permanence which is reminiscent of the permanent correlation existing in a solid.

IV. NON-GAUSSIAN BEHAVIOR OF $G_s(r,t)$

If $G_s(r,t)$ has the Gaussian form, $[4\pi\rho(t)]^{-3/2}\times\exp[-r^2/4\rho(t)]$, one has the following relations:

$$\langle r^2\rangle=6\rho(t),$$
$$\langle r^{2n}\rangle=C_n\langle r^2\rangle^n,$$
$$C_n=1\times3\times5\times7\cdots(2n+1)/3^n,$$

for $n=1, 2, 3, \cdots$. Thus, a departure of $G_s(r,t)$ from a Gaussian form can be expressed in terms of the functions, $\alpha_n(t)$, defined by

$$\alpha_n(t)=(\langle r^{2n}\rangle/C_n\langle r^2\rangle^n)-1.$$

For a non-Gaussian $G_s(r,t)$ the α_n, $n=2, 3, \cdots$ will not vanish.

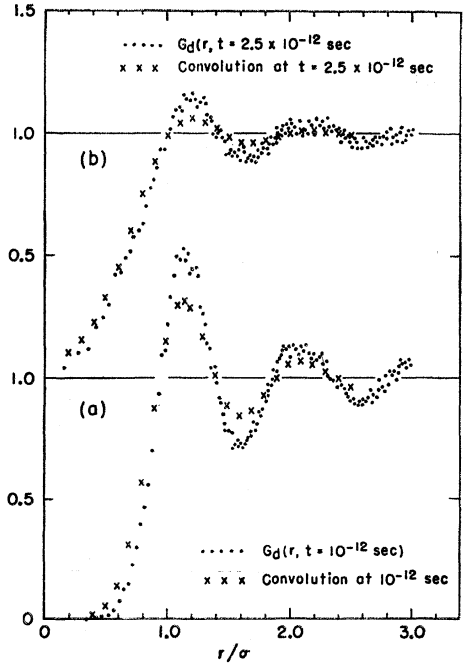

FIG. 6. Time-dependent pair-correlation function $G_d(r,t)$ shown at two values of t. The convolution approximation of Vineyard (Ref. 6) gives a too rapid decay of G_d.

[4] J. Naghizadeh and S. A. Rice, J. Chem. Phys. **36**, 2710 (1962).

In Fig. 7 we have shown α_2, α_3, and α_4. Since the values are all positive, we conclude that G_s goes to zero with increasing r more slowly than a Gaussian. The flatness of the curves near the origin reflects the Maxwellian distribution of velocities, because at short times $\langle r^{2n}\rangle$ tends to $\langle v^{2n}\rangle t^{2n}$.

As $t\to\infty$ the non-Gaussian behavior of $G_s(r,t)$ should disappear. Figure 7 shows that $\alpha_2, \alpha_3, \alpha_4$ start to decrease after 3.0×10^{-12} sec. By extrapolating the curves to the right, one can roughly put down 10^{-11} sec as the time when G_s becomes Gaussian again. At $t=10^{-11}$ sec, the value of $\langle r^2\rangle^{1/2}$ is 3.8 Å, and this is very nearly equal to the first-neighbor distance of 3.7 Å (Fig. 2).

The non-Gaussian behavior of $G_s(r,t)$ can be expressed alternatively by expanding the function in a series of $\mathrm{He}_{2n}(x)$, the even Hermite polynominals[5]; it is straightforward to show that the coefficients in the expansion,

$$G_s(r,t)=[4\pi\rho(t)]^{-3/2}\exp[-r^2/4\rho(t)]\times\{1+b_6(t)\mathrm{He}_6(\alpha r)+b_8(t)\mathrm{He}_8(\alpha r)+\cdots\},$$

with $\alpha^2=3/\langle r^2\rangle$, are given in terms of the $\alpha_n(t)$ by

$$6b_6=(3/4!)\alpha_2(t),$$
$$b_6+8b_8=(3\times5/6!)\alpha_3(t)-(3/2\times4!)\alpha_2(t),$$
$$b_8+10b_{10}=(3\times5\times7/8!)\alpha_4(t)-(3\times5/2\times6!)\alpha_3(t)+(3/2^2\times2\times4!)\alpha_2(t),$$

etc. To illustrate the situation let us substitute the values of α_2, α_3, α_4 at $t=2.5\times10^{-12}$ sec (see Fig. 7). Putting $\alpha_2=0.13$, $\alpha_3=0.40$, $\alpha_4=0.83$ we get $b_6=0.0027$, $b_8=-0.0003$, and $b_{10}=0.00003$, showing that the first few terms in the expansion above give a good description of the non-Gaussian behavior of G_s. In fact the values of $\alpha_2, \alpha_3, \alpha_4$ are such that we essentially have $b_6+8b_8\approx0$ and $b_8+10b_{10}\approx0$.

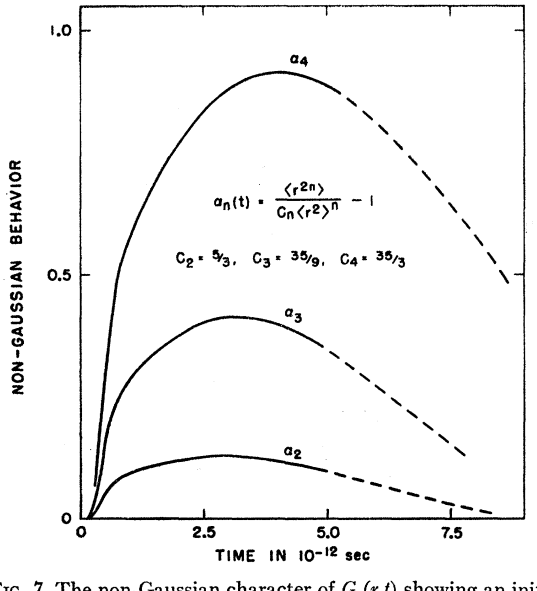

FIG. 7. The non-Gaussian character of $G_s(r,t)$ showing an initial Gaussian behavior lasting about 0.15×10^{-12} sec and, on extrapolating to the right, a return to a Gaussian form at about 10^{-11} sec. Maximum departure of $\langle r^4\rangle$ from its Gaussian value is only about 13%.

[5] *Tables of Integral Transforms, Bateman Manuscript Project*, edited by H. Erdelyi (McGraw-Hill Book Company, Inc., New York, 1954).

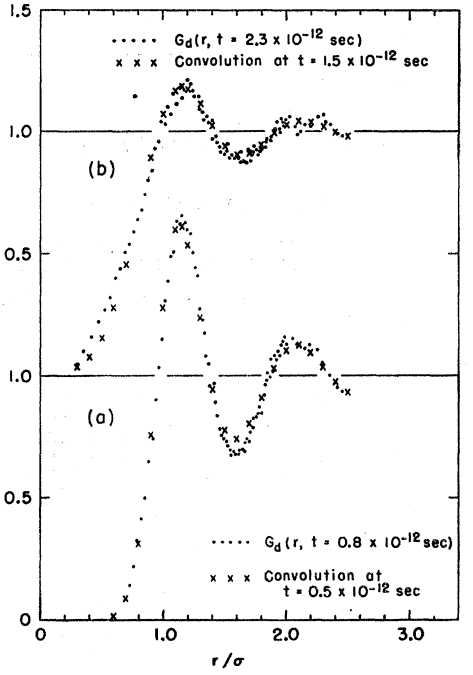

FIG. 8. $G_d(r,t)$ is compared with the convolution of $g(r)$ and $G_s(r,t')$ with $t'<t$, for two pairs of values of t and t' showing the extent to which such a delayed convolution improves the Vineyard approximation (Fig. 6).

V. THE CONVOLUTION APPROXIMATION OF VINEYARD

To describe the time dependence of $G_d(r,t)$, Vineyard[6] has suggested an approximation which makes G_d a convolution between $g(r)$ and $G_s(r,t)$. Following Vineyard one first writes the formal equality

$$G_d(\mathbf{r},t)=\int g(\mathbf{r}')H(\mathbf{r}-\mathbf{r}',t)d\mathbf{r}',$$

where $H(\mathbf{r}-\mathbf{r}',t)$ is the probability that the particle at $\mathbf{r}'$ travels to $\mathbf{r}$ in time t, given that another particle was situated at the origin at $t=0$.

Vineyard's approximation consists in putting $H=G_s$ in the above equation. However, the motions of particles in the first shell are strongly correlated with the occupation of the origin by another particle at $t=0$, and Vineyard's approximation overlooks this fact. In other words, the approximation leads to a too rapid decay of $g(r)$. This is shown in Fig. 6 where the actual $G_d(r,t)$ and the Vineyard approximation are compared at $t=10^{-12}$ sec, and at $t=2.5\times10^{-12}$ sec.

[6] G. H. Vineyard, Phys. Rev. **110**, 999 (1958).

From this it follows that the Vineyard approximation might be improved by delaying the convolution in the following way. We write

$$G_d(\mathbf{r},t)=\int g(\mathbf{r}')G_s(\mathbf{r}-\mathbf{r}',t')d\mathbf{r}',$$

where the delayed time $t'(t)$ is always earlier than t. When t is small we should have $t'\rightarrow t^2$, so that at small times G_d starts decaying as t^4 as it should and not as t^2 as in the Vineyard approximation. When t is large we should have $t'\rightarrow t$.

By matching G_d obtained by a convolution at time t' with the actual G_d at time t, one finds the following pairs (t',t) in units of 10^{-12} sec: (0.2,0.4), (0.5,0.8), (1.0,1.6), (1.5,2.3), (2.0,2.9), (2.5,3.5). Figure 8 shows two examples of how a convolution at $t'<t$ fits the G_d at t. This can be described as a functional relation between t' and t, and the following is suggested as a simple one-parameter function:

$$t'=t-\tau[1-\exp(-t/\tau)-(t^2/\tau^2)\exp(-t^2/\tau^2)].$$

With $\tau=1.0\times10^{-12}$ sec one gets the pairs of values (0.21,0.4), (0.59,0.8), (1.0,1.6), (1.4,2.3), (2.0,2.9), (2.5,3.5).

There are two points to be clearly stated here. Firstly, a delayed convolution will certainly be an improvement over the Vineyard approximation; secondly, in the light of the results obtained in our calculations an empirical functional form for the delay has been suggested involving just one parameter τ.

If we denote the Fourier transform of $G_d(r,t)$ by $F_d(\kappa,t)$ and of $G_s(r,t)$ by $F_s(\kappa,t)$, the delayed convolution gives $\gamma(\kappa)F_s(\kappa,t')$ as an approximation for $F_d(\kappa,t)$ instead of the Vineyard approximation $\gamma(\kappa)F_s(\kappa,t)$. The extent to which this gives an improvement is being investigated.

VI. CONCLUSIONS

A classical 864-body problem with a truncated two-body interaction of the Lennard-Jones type, with periodic boundary conditions is, by itself, a problem of interest, in which case the assumptions involved reduce simply to the assumptions in solving the set of differential equations as a set of difference equations.

The question of identifying such a system with a physical system like liquid argon is very difficult to answer on the basis of the limited amount of information presented in this paper. Firstly, the value of the diffusion constant obtained here is in good agreement with the observed value; this is some justification for saying that the time-dependent mean-square displacement $\langle r^2\rangle$ obtained here is correct; in that case the non-Gaussian behavior of $G_s(r,t)$ shown above should also be dependable. Secondly, the function $g(r)$ we have calculated is in good agreement with the observed pair-distribution function and the $G_d(r,t)$ obtained here differs from that obtained with the Vineyard approximation in the right direction; this has enabled us to suggest an improvement over the Vineyard approximation which can be checked by using neutron scattering data.

A more stringent test for the validity of a model for self-diffusion is the dependence of the diffusion constant on temperature. A calculation of the type described above at 130°K and 1.16 g cm^{-3} gave a diffusion constant $D=5.67\times10^{-5}$ cm^2 sec^{-1}. The experimental value of Naghizadeh and Rice[4] at 120°K and 1.16 g cm^{-3} is $D=6.06\times10^{-5}$ cm^2 sec^{-1}. Thus the variation of D with temperature and density is also in fairly good agreement with the variation measured in the laboratory. It should be noticed, however, that our calculated values are in both cases lower than those measured in the laboratory by about 20%. Calculations are now being made to check if this discrepancy can be reduced by allowing for a softer repulsive part in the interaction potential.

ACKNOWLEDGMENTS

The author wishes to thank Dr. Lester Guttman for many useful discussions during the progress of the work and for invaluable help in the preparation of this paper. The unrelenting patience and cooperation of the scheduling and operating personnel of the CDC 3600 at Argonne are most thankfully acknowledged.

APPENDIX

If x_i and v_i are the components of the position and velocity of the particle i in any direction we have

$$dx_i/dt=v_i, \tag{1}$$

$$\frac{dv_i}{dt}=a_i=24\frac{\epsilon}{M}\sum_{j\neq i}\frac{x_i-x_j}{r_{ij}^2}\left\{2\left(\frac{\sigma}{r_{ij}}\right)^{12}-\left(\frac{\sigma}{r_{ij}}\right)^{6}\right\}. \tag{2}$$

Taking σ as the unit of length and $(\epsilon/M)^{1/2}$ as that of velocity and using dimensionless variables ξ, η, u, ρ, and α for x, v, t, r, and a we have

$$d\xi_i/du=\eta_i, \tag{3}$$

$$\frac{d\eta_i}{du}=\alpha_i=24\sum_{j\neq i}\frac{\xi_i-\xi_j}{\rho_{ij}^2}\left\{\frac{2}{\rho_{ij}^{12}}-\frac{1}{\rho_{ij}^{6}}\right\}. \tag{4}$$

Corresponding to an interval $\Delta t=10^{-14}$ sec we have an interval $\Delta u=10^{-14}(\epsilon/M)^{1/2}(1/\sigma)$.

Let us assume that we are given the positions $\xi_i^{(n-1)}$ at time u_{n-1} and the positions, velocities and accelerations $\xi_i^{(n)}$, $\eta_i^{(n)}$ and $\alpha_i^{(n)}$ at time $u_n=u_{n-1}+\Delta u$.

Using a predictor formula for positions $\bar{\xi}$ at time u_{n+1}, we have

$$\bar{\xi}_i^{(n+1)}=\xi_i^{(n-1)}+2\Delta u\eta_i^{(n)}.$$

With these we get predicted accelerations $\bar{\alpha}_i^{(n+1)}$ using Eq. (4). Using these we get the new positions and velocities

$$\eta_i^{(n+1)}=\eta_i^{(n)}+\tfrac{1}{2}\Delta u(\bar{\alpha}_i^{(n+1)}+\alpha_i^{(n)}),$$
$$\xi_i^{(n+1)}=\xi_i^{(n)}+\tfrac{1}{2}\Delta u(\eta_i^{(n+1)}+\eta_i^{(n)}).$$

This process can be repeated until the predicted and corrected values of $\xi_i^{(n+1)}$ differ by less than a prescribed value. However, the procedure adopted was to make trial runs on the system of 864 particles with one and with two repetitions of this predictor-corrector procedure. A comparison of the results in terms of the correlations discussed in this paper showed no observable difference. As a further check, the motion of a diatomic system was calculated with one and with two repetitions of this procedure. The two particles were initially at a distance $\rho_{12}=1.9$ and were allowed to oscillate; their positions at 2000 successive intervals Δu were recorded covering a little over three periods of oscillation and the following is a summary of the results to show the degree to which the approximations involved in using the difference equations affect the motion.

(a) At the end of three successive oscillations the separations were: 1.8958, 1.8932, 1.8890, when the predictor-corrector procedure was used only once and 1.9018, 1.9016, and 1.9044 when it was used twice, thus giving improved results.

(b) The distance of closest approach was successively 1.0039, 1.0040, 1.0041 in the first case and 1.0038, 1.0038, 1.0038 in the other.

(c) The mean-square velocity in °K while going through the minimum of the potential was 36.65, 36.61, 36.60, 36.59, 36.59, 36.54, in one case and 36.65, 36.67, 36.67, 36.68, 36.67, 36.70, in the other.

(d) The period of oscillation was (in units of 10^{-12} sec) 6.27, 6.22, 6.17, in one case, and 6.31, 6.32, 6.33 in the other.

This gives an idea of the errors involved in using the difference equations given above. The results given in the paper were all obtained in a run with two passes through the predictor-corrector procedure.

There are five factors which determine the time for computing one step Δu, namely, N, R, the number of predictor-corrector cycles, the manner of writing the program, and the computer used. For $N=864, R=2.25\sigma$, using floating point arithmetic each cycle takes 45 sec on the CDC-3600 computer. For $N=250$, $R=2.0\sigma$, using fixed point arithmetic each cycle takes 40 sec on the IBM-704 machine. For the most time consuming part the program was written in machine language and in FORTRAN for the rest.

PHYSICAL REVIEW VOLUME 136, NUMBER 2A 19 OCTOBER 1964

Interactions Between Elastic Waves in an Isotropic Solid*

J. D. CHILDRESS AND C. G. HAMBRICK†
Department of Physics and Astronomy, Louisiana State University, Baton Rouge, Louisiana
(Received 18 May 1964)

Interactions between elastic waves in an isotropic solid are studied in the elastic-continuum approximation. The analysis is carried out completely in a wave-packet formalism, i.e., scattering of wave packets by wave packets. The maximum amplitude (or intensity) and width of the scattered wave packet are expressed in terms of the maximum amplitudes, frequencies, widths, polarizations, and relative propagation directions of the primary-wave packets. The polarization relations and frequency ranges for the allowed interaction processes are obtained; these are essentially identical to the ones given by Jones and Kobett. The results are shown to be in good order-of-magnitude agreement with the experiments of Rollins. Possible application of elastic-wave scattering to the determination of third-order elastic constants is discussed.

I. INTRODUCTION

ELASTIC waves in solids have attracted much theoretical and experimental interest; but surprisingly, the interaction between elastic waves (phonon-phonon scattering) has been investigated experimentally only recently. Last year, Rollins[1] observed directly the production of "sum" and "difference" frequency waves from the interaction of two ultrasonic pulses in aluminum. Somewhat earlier, Gedroits and Krasil'nikov[2] demonstrated the effects of such interactions on the attenuation and harmonic distortion of an ultrasonic wave interacting with itself. Mahler, Mahon, Miller, and Tantilla[3] and Shiren[4] later reported observations of the same phenomena by different experimental means. At about the same time, Jones and Kobett[5] (classical approach) and Childress and Fried[6] (quantum-mechanical approach) discussed elastic-wave interactions and found that such processes should indeed be experimentally observable.

* Part of this work was submitted by C. G. H. in partial fulfillment of the requirements for the M.S. degree at Louisiana State University.

† Present address: Department of Physical Sciences, McNeese State College, Lake Charles, Louisiana.

[1] F. R. Rollins, Jr., Appl. Phys. Letters **2**, 147 (1963).

[2] A. A. Gedroits and V. A. Krasil'nikov, Zh. Eksperim. i Teor. Fiz. **43**, 1592 (1962) [English transl.: Soviet Phys.—JETP **16**, 1122 (1963)].

[3] R. J. Mahler, H. P. Mahon, S. C. Miller, and W. H. Tantilla, Phys. Rev. Letters **10**, 395 (1963).

[4] N. S. Shiren, Phys. Rev. Letters **11**, 3 (1963).

[5] G. L. Jones and D. Kobett, J. Acoust. Soc. Am. **35**, 5 (1963). An erratum notes the omission of a term

$$-(K-\tfrac{2}{3}\mu+B)[(\mathbf{A}_0\cdot\mathbf{k}_1)(\mathbf{k}_1\cdot\mathbf{k}_2)\mathbf{B}_0\pm(\mathbf{B}_0\cdot\mathbf{k}_2)(\mathbf{k}_1\cdot\mathbf{k}_2)\mathbf{A}_0]$$

in the expression for $\mathbf{I}^{\pm}$ below Eq. (4) (their notation).

[6] J. D. Childress and Z. Fried, Bull. Am. Phys. Soc. **8**, 16 (1963).